Making 5G Millimeter Wave Communications a Reality

A. De Domenico, R. Gerzaguet, N. Cassiau, A. Clemente, R. D'Errico, C. Dehos, J. L. González, D. Kténas, L. Manat, V. Savin, and A. Siligaris

CEA LETI, Minatec Campus, 17 rue des Martyrs, 38054, Grenoble, France

Grenoble-Alpes University, 38000, Grenoble, France

Introduction

Driven by the data requirements envisioned for the 5th generation (5G) of wireless services, the mobile community is focusing on breaking the spectrum gridlock that characterizes the cellular technology. In this context, researchers and industries have identified millimeter-wave (mmWave) communications as a key enabler for providing unprecedented radio access capacity. Nevertheless, due to the specific differences between this technology and the microwave systems, there exist multiple research challenges spanning from the hardware to the overall system architecture. The goal of this article is to provide an overview of these challenges and discuss the most promising solutions to make 5G mmWave communications a reality.

An overview of mmWave Spectrum

In opposition to the below 6 GHz spectrum, mmWave bands may provide the opportunity for large portion of globally available frequencies, including licensed, lightly licensed, and unlicensed spectrum. In particular, within this spectrum, the main research efforts are oriented on the so-called Ka band (27.0 – 40.0 GHz), V band (57-64 GHz), and E band (71-76 and 81-86 GHz). In 2015, the International Telecommunication Union proposed a list of worldwide viable mmWave frequencies [1]. More recently, the Federal Communications Commission has allocated about 11 GHz of mmWave spectrum for 5G services in United States. In addition, key mobile vendors are currently developing mmWave prototypes to showcase their technologies before 2020. In these testbeds, the frequency bands around 28, 39, and 72 GHz have emerged as candidate solutions to demonstrate the 5G mmWave hardware. To conclude, beside standardization and industry activities, the wireless research community is looking beyond the 100 GHz band, to investigate the solutions that will enable to reach the target of 100 Gbps communications.

What Technology to select for the mmWave RF Transceiver?

The recent advances in mmWave electronics have enabled significant portions of the Radio Frequency Front End (RFFE) to be integrated onto a single substrate or package. To achieve low cost and high integration along with digital circuitry, silicon based CMOS

or BiCMOS process technologies are utilized. CMOS is a standard and cost effective process for building digital circuits, and CMOS 65, 45, and 40 nm technologies have demonstrated their maturity for 60 GHz WiGig and 77-81 GHz automotive radar applications [2]. Indeed, as technology scales down for CMOS process, the transit frequency, f_T, and unity power gain frequency, f_{max}, grow steadily and are approaching a few hundreds of GHz for advances nodes, reaching 300 GHz for the n-MOSFET at the 28nm node. This is comparable to more expensive technologies based on III-V semiconductor compounds, such as InP and Gallium Arsenide (GaAs). Starting with 130-nm SiGe BiCMOS node, designers can take advantage of the comparable n-MOSFET and SiGe HBT speed for the realization of high-frequency, low-voltage, and low-power mmWave Integrated Circuits (ICs) in the 28-80 GHz range.

To summarize, the requirements for a semiconductor technology to be well suited for mmWave integrated transceiver design could be listed as:

- f_T and f_{MAX} should be at a minimum 3x and preferably >5x the application frequency.
- Low loss back end of line in term of substrate resistivity, top metal thickness, and distance from substrate.
- Very good CAD process device modeling and parasitic extraction methods to minimize design iterations.
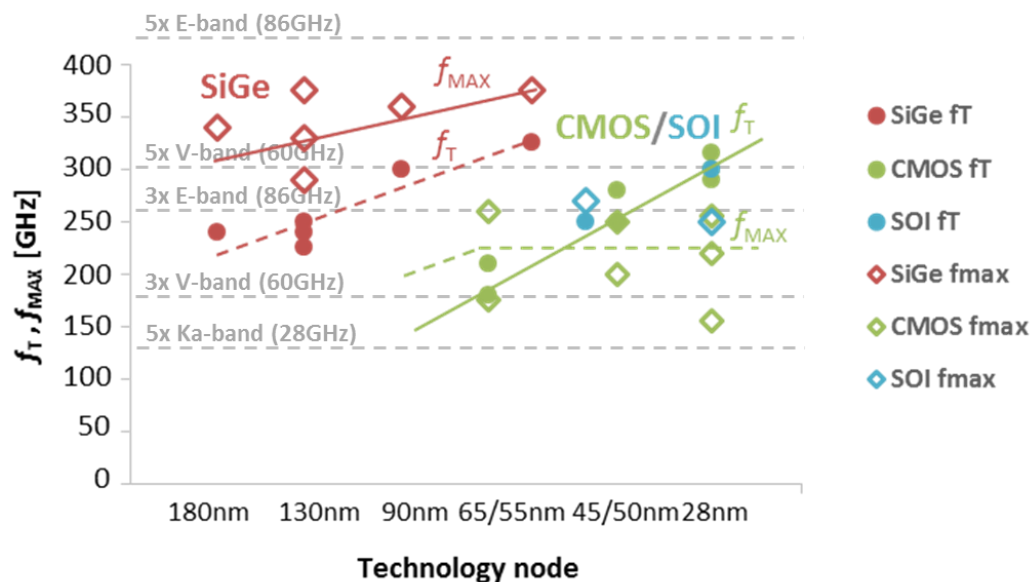- Low cost of manufacturing and integration scale.

Figure 1: Matching between silicon based technologies and mmWave transceivers.

Figure 1 compares the silicon based technology performances in terms of f_T and f_{MAX} with respect to the requirements for the different frequency bands considered in 5G small-cell systems, showing that silicon technologies are able to cover all of them.

To conclude, the performance of the CMOS or SiGe transistors is no longer the limit for

an mmWave transceiver front end integration but this is mainly limited by the impact of the operating frequency on the quality factor of the on-chip passive devices as well as their accurate characterization. Advanced BiCMOS and CMOS-SOI processes offer 5-10 interconnect metal layers (inherited from digital technologies) that may be adapted to design low loss, compact integrated waveguides, and other passives by adding extra top thick metal layers, with typical 3μm thickness at a the distance from the substrate of about 6μm.

Radio Frequency Front-End Design

Compared with III-V technologies, silicon-based technologies give greater process variability, lower carrier mobility constants, and smaller device breakdown voltages. Nevertheless, cost, power consumption, and relative performance are well suited for mobile terminal transceivers. However, at the access side, silicon-based design is particularly challenging since 5G small cells requires flexible beam-forming and beam-steering capabilities. We have recently developed a 60 GHz compact antenna array able to synthesize various beams, each one serving a distinct user, by combining a single CMOS RFFE Tx/Rx IC and dedicated SiGe BiCMOS active phase shifter ICs for each of the antenna sub-arrays. In addition to directive antennas, high output Power Amplifiers (Pas) (P1dB ~15-20 dBm) are required to achieve link distances of up to 100m [3]. PAs based on 40nm CMOS and power combining techniques can provide up to 15.6 dBm of P1dB while recent realizations in FDSOI 28nm CMOS have achieved up to 18.2 dBm, indicating that fully integrated silicon mmWave transceivers for 5G small cells are a feasible solution.

Concerning the user terminal, we have combined the 60 GHz transceiver with patch antennas integrated in a high performance ceramic substrate to achieve 7 dBi of antenna gain including interconnection loss (see Figure 2) [2]. Two main alternatives exist for the (de)modulation stage in the RF transceiver: a direct conversion architecture or a heterodyne architecture. The direct conversion solution requires local oscillator providing two different phases (0º and 90º) at the same frequency of the RF channel, which is very challenging. The choice of the Voltage Control Oscillator (VCO) frequency and, in general, of the frequency plan, is indeed a crucial step in the design of the mmWave RFFE. It turns out that the best performance in terms of phase noise limitation is obtained when the integrated VCO tank passives operate at their peak quality factor (around 20 GHz). Therefore, the most suitable architecture is based on heterodyne up/down conversion.
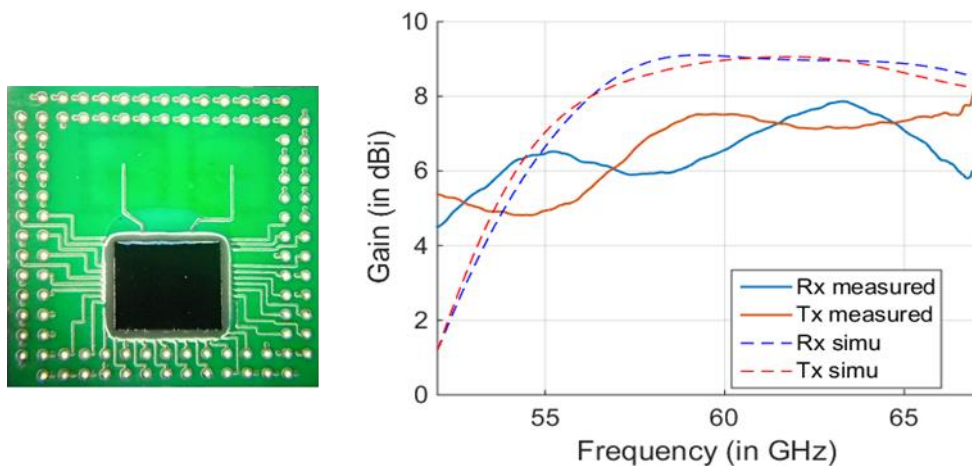
Figure 2: (Left) fabricated module with flip-chipped mmW Rx/Tx transceiver; (Right) User Terminal antenna gain.

Reconfigurable High Gain Antennas for the mmWave Small Cell

As already mentioned, the small cell antenna requires around 20-30 dBi gains to compensate the propagation losses and the relative low antenna gain at the end terminal. It also needs to implement flexible beam-steering to follow users moving nearby the mmWave small cell. In this section, we present two different antenna architectures, based respectively on hybrid and analog beamforming, capable to deal with these technical challenges: (i) a phased array antenna with multi-beam capability and (ii) a transmitarray antenna with 2D beam-steering capabilities.
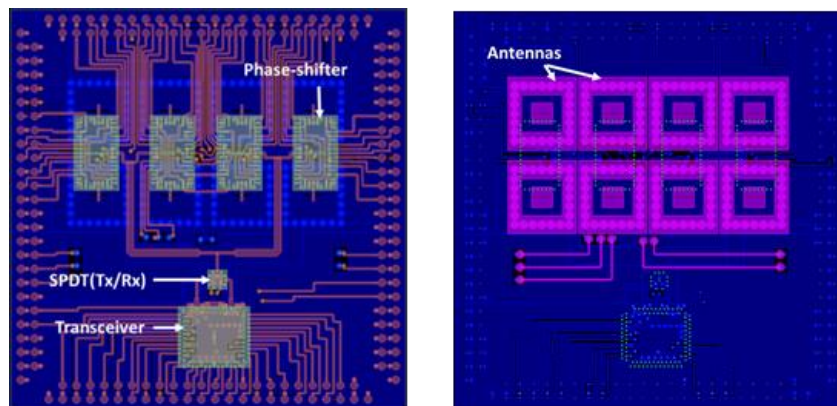

Figure 3: Layout of a sub-array in the phased array antenna.

We develop a phased array antenna composed of 2×4 sub-arrays, which corresponds to 4×16 radiating elements. Our analysis shows that the radiation patterns for a single sub array ranges from 16.9 dBi to 17.7 dBi. This architecture enables either to assign each sub-array to a different user or to synchronize several sub-arrays that coherently form a single beam with up to 26.6 dBi gain. In the first case, each user may be allotted to a dedicated frequency channel according to a frequency-division multiple access policy; the latter approach enables the small cell to provide reliable access to cell-edge users or to further enhance the data rate of closer users.

Figure 3 shows the layout of a sub-array including the RF transceiver connected to the antenna array through a Tx/Rx switch and phase-shifter ICs. The phase shifter enables to steer the antenna beam by adjusting the phase between adjacent antenna elements: this solution, at 60 GHz, enables a maximum steering angle of 60°.

The transmitarray with beam-scanning capability is composed of four principal blocs: (i) the digital processing unit, (ii) the RF transceiver, (iii) the focal source, and (iv) the electronically steerable flat-lens. The principle of a transmitarray antenna is similar to the one of an optical lens. The quasi-spherical electromagnetic wave radiated by the focal source is focalized or collimated in a given direction by adjusting the transmission phase of each element (called unit-cell) of the flat-lens. Electronically beam-scanning capability can be achieved by tuning the transmission phase of an active unit-cell by integrating e.g., varactors or p-i-n diodes. The transmitarrays can handle more power with enhanced linearity than the phased array and also can reduce the power loss in the phase-shifter network thanks to the integration of the spatial feeding technique. As a consequence, this technology is an excellent candidate for the implementation of large mmWave array.

First, we used this architecture for developing a reconfigurable transmitarray working around 10 GHz [4]. The linearly-polarized flat-lens is composed of 20×20 unit-cells with 1-bit of phase quantization (two phase-states 0° or 180°). Each unit-cell is composed of two rectangular microstrip patch antennas loaded by a slot whose transmission phase is controlled by using two p-i-n diodes integrated on one of the patch. The flat-lens is illuminated by a 10-dBi standard gain horn. The antenna demonstrates experimentally pencil beam scanning over a 140×80-degree window, with a maximum gain of 22.7 dBi [4].
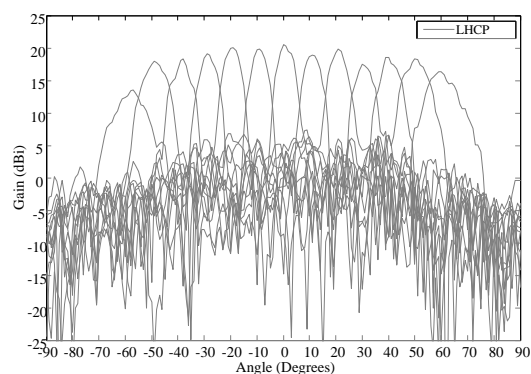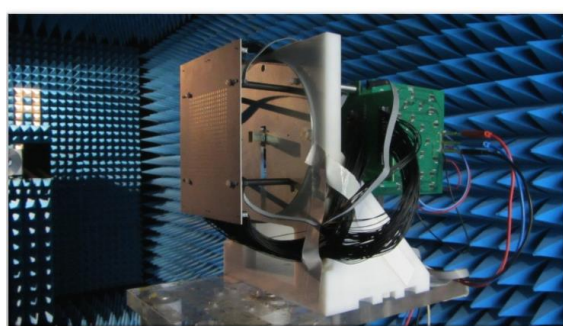

Figure 4: (Left) Photograph of the circularly-polarized electronically reconfigurable transmitarray at 29 GHz; (Right) Measured radiation pattern as a function of the scanning angle.

Then, we have developed a 400-element electronically reconfigurable transmitarray working in circular polarization around 29 GHz (see the left-side of Figure 4) [5]. This array is based on a unit-cell architecture [6] where the circular polarization is achieved by sequentially-rotating the patch antennas located on the transmission layer of the

flat-lens. We also demonstrated left-hand / right-hand circular polarization switching and 2D electronic beam-steering capabilities of ±60°, which is obtained by controlling the p-i-n diodes integrated on the flat-lens aperture. The prototype, illuminated by a 10-dBi standard gain horn antenna as a focal source, exhibits a broadside gain of 20.8 dBi.

Analogue, Digital, or Hybrid Beamforming?

Analog beamforming is a technology used to provide the high gain antennas required by mmWave communications. In this solution, a single Baseband (BB) and Radio Frequency (RF) chain feeds an array of transmit antennas; by modifying the phase of each antenna and the array topology (e.g., the element spacing), several beams with desired width and power are created. This approach is of particular interest at mmWave frequencies, where very compact antennas with large number of elements can be designed but it suffers from several constraints. The first one is the limitation on the phase resolution of antennas, which is typically $n\pi/2, n \in \mathbb{N}$. The limited set of phases reduces the number of beams and, therefore, the resolution of the scan angle. The second constraint, predominant in an access link scenario, is the latency of the system: the optimal beam has to be refreshed each time the channel changes significantly. This operation may be realized very frequently when the user is moving and / or when the number of available beams is high. In the 802.11ad standard, dedicated sequences are used to select and refine the beams. This approach simplifies the beam control at the cost of a net rate loss [7]. Researchers are currently focusing on designing solutions that decrease the time required for the choice of the optimal beams.

In contrast to analog beamforming, in digital beamforming the numerical treatments are realized in the BB and the N outputs of the BB feed N RF chains and N antennas. The BB computations involve the channel matrix or more realistically a partial estimate of it. The goal of digital beamforming is to serve several users in the same time-frequency resources with minimum perceived interference. If this process theoretically allows high resource gains, some limitations appear when it comes to a real implementation. First, the power consumption of RF components makes the use of very large antenna arrays prohibitive. Moreover, the accuracy of BB algorithms requires a large amount of signaling related to the channel state information. Finally, BB processing typically need high computational and memory capabilities.

The hybrid beamforming combines analog and digital beamforming: it mixes the BB computational capacities of digital beamforming and the possibility to create beams allowed by the analog beamforming. It is a promising technique for mmWave multiuser scenarios that enables to use larger beam for each user (hence decreasing the system latency due to beam search) and to null the inter-user interference, due to

beams overlapping, at the BB level. CEA LETI is currently focusing on demonstrating multiuser hybrid beamforming for mmWave systems.

Characterize and Model mmWave Channel

Define comprehensive and rigorous channel models of the entire mmWave range able to cover all relevant usage scenarios is one of the key challenge for further development of 5G systems. In the past, most of the research effort related to mmWave propagation has been on short-range indoor communications in the unlicensed 60 GHz frequency band.

Today, with the increasing attention drawn with the development of the 5G, academic and industry have obtained relevant experimental results on this field. Their promising conclusion is that not only broadband *line-of-sight* (LOS) links can be supported, as reflections from the ground, buildings, and smaller objects can often be exploited to realize non-LOS (NLOS) transmissions. More specifically, Qualcomm ray-tracing experiments at 28 GHz have demonstrated that in urban outdoor deployment ~150 m coverage can be achieved by jointly using LOS and NLOS links. In other terms, this proves that mmWave technology can be used to provide mobile outdoor services.

As a consequence of these results, during the last few years, an intensive work has been carried out for developing and designing accurate channel models.

A notable outcome is the IEEE channel model developed for the IEEE 802.11ad and IEEE 802.15.3c standards. Furthermore, the New York University has conducted many urban propagation measurements on 28/38/60/73 GHz bands for both outdoor and indoor channels. Important experimental and modeling activities have taken place in the EU projects MiWEBA and mmMagic. Specifically, MiWEBA developed a 60 GHz 3D channel model for outdoor/indoor access and backhaul scenarios while mmMagic is undertaking extensive radio channel measurements in the 6-100 GHz range to accurately model blockage, spatial consistency, intra-cluster characteristics, and ground reflections. Finally, the 3rd generation partnership project is currently developing channel models for enabling system level simulations at mmWave frequencies [8].

Some challenges still exist in modelling the mmWave radio environment, in particular, concerning the characterization of outdoor environments, mobility, and use cases related to vertical industries. CEA LETI has performed indoor double directional measurements at 60 and 82 GHz in office and conference rooms [9]. We have characterized pathloss, delay, and angular spreads by detecting propagation paths in the angular and delay domains. In addition, these experiments have included measurements for human blockage. In the future, we aim to assess the channel characteristics in highly dynamic conditions as well as the antenna effect on the overall channel properties. To this purpose, we plan channel measurement in V2X scenarios,

including double-mobility, and trials with real beamforming antennas.

Optimized waveforms for mmWave communications

The waveform design for mmWave communications faces a number of challenges, especially due to the path loss and the potential strong doppler effect for mobile users. Besides, due to the high carrier frequency, the hardware used for mmWave transmitter faces many imperfections. To unleash very high data rates and high spectral efficiency, waveforms should be optimized to support massive MIMO and the use of large antenna arrays.

In the past decades, many single carrier (SC), and multicarrier (MC) waveforms have been developed for wireless communications, each with its pros and cons. Although there is no single optimal waveform for all scenarios, it is possible to optimize the waveforms with respect to some key requirements.

Despite their high Peak to Average Power Ratio (PAPR), MC enables higher spectral efficiency and better modularity as compared to SC waveforms. With the addition of pre-coding techniques and/or PAPR reduction methods, power efficient MC systems can be designed. MC waveforms offer also simple equalization scheme and are suitable to MIMO and beamforming.
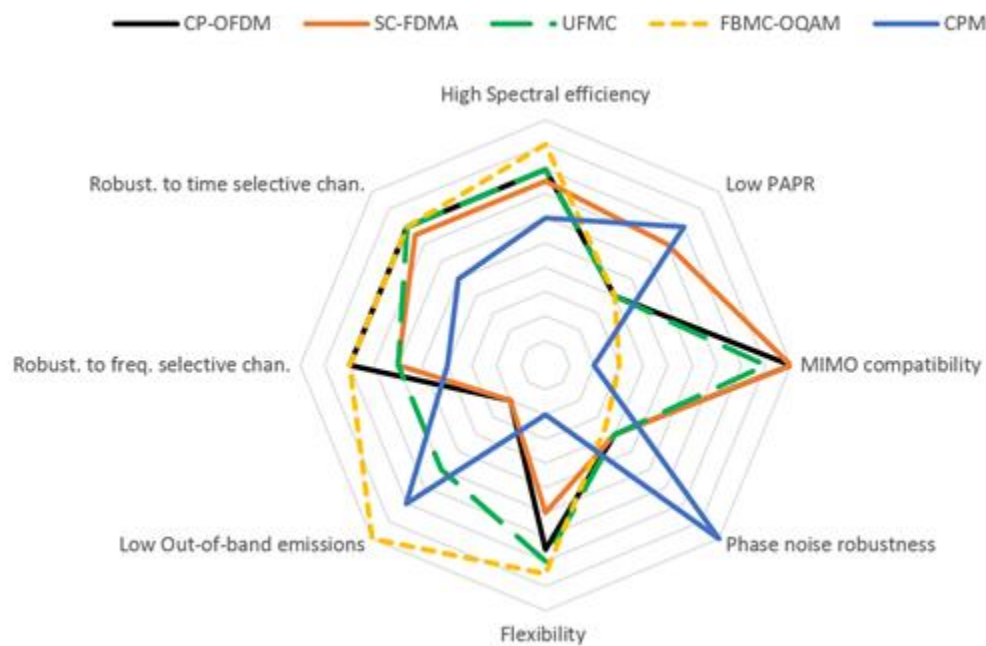

Figure 5: Waveform comparison in terms of key performance indicator.

Generally, some waveforms can be identified as the most promising candidates for mmWave scenarios (see Figure 5) [10]. Among them, legacy Cyclic Prefix Orthogonal Frequency Division Multiplexing (CP-OFDM), used in current LTE downlink system, and Single Carrier Frequency Division Multiple Access (SC-FDMA), used for LTE uplink, are on the race for mmWave scenarios. Universal Filtered OFDM (UF-OFM) is a new

multicarrier waveform that performs an additional filtering stage on the transceiver. Filter Bank Multicarrier, a modulation scheme where the subcarriers are shaped by a scalable prototype filter, offers a good alternative due to its very good frequency location at the detriment of a straightforward MIMO solution. On the contrary, SC waveforms, such as Constant Phase Modulation (CPM), offer good resistance against hardware impairments and a low PAPR but flexibility and MIMO compatibility are currently an issue.

FEC mechanisms for very massive data rate

Massive data rates will require significantly higher processing speed of the BB signal, as compared to conventional solutions. This is especially challenging for Forward Error Correction (FEC) mechanisms, which consumes a large amount of hardware resources and energy. The use of very large bandwidths will result in stringent, application-specific, requirements for the decoder in terms of throughput and latency. The conventional approach to increase the decoder throughput is to use massively parallel architectures. Low-Density Parity Check (LDPC) and Turbo codes stand as natural candidate solutions, since they both may accommodate various degrees of parallelization and are already in use in many wireless standards. Although Turbo codes have the advantage of ensuring backward compatibility with LTE-Advanced, LDPC codes provide more flexibility in terms of code design and hardware architectures, thus being particularly relevant to massive data rates systems. Table I provides a comparison between state-of-the-art high throughput implementations of LDPC and Turbo decoders, for various wireless standards.

Table 1: State-of-the-art high throughput HW implementations of LDPC and Turbo decoders.

Authors	Ilnseher2012	Shrestha2014	Zhang2009	Kumawat2015	Schlafer2013	Truong2016
Code type	Turbo	Turbo	LDPC	LDPC	LDPC [11]	LDPC[12]
Standard / or Code Family	LTE-A	LTE-A	802.16e (WiMAx)	802.11n (WiFi)	802.11ad (WiGig)	(3,6)-regular
Max. Block-Length	6144	6144	2304	1944	672	1296
Parallelization Degree	32	64	12	81	fully parallel	54
Nb. Iterations	6	6	10	10	9	10
Technology (nm)	**65**	**90**	**90**	**90**	**65**	**65**
Frequency (MHz)	450	625	950	336	257	250
Core Area (mm²)	7,7	19,75	2,9	5,2	12,09	0,72
Power (mW)	--	1450,5	870	451,3	5360	--
Throughput (Gbps)	**2,15**	**3,03**	**2,20**	**1,71**	**160,80**	**5,40**
Latency (ns)	**2857,7**	**2027,7**	**1047,3**	**1136,8**	**105,0**	**240,0**

Normalized Energy, Throughput and Latency, after technology scaling to 65 nm

Energy eff. (pJ/bit)	--	180,34	148,97	99,42	33,33	--
Area eff. (Gbps/mm²)	0,28	0,41	2,01	0,87	13,30	7,50
Norm. Latency (ns/bit)	0,47	0,24	0,33	0,42	0,16	0,19

The parallelization degree reported in the table refers to the number of processing units operating in parallel. Decoding latency is inversely proportional to the decoder throughput, except for the parallel LDPC decoder architecture [11], for which the iterative decoding loop is fully unrolled in hardware and pipelined. Hence, this architecture has a throughput of one codeword per clock cycle, while decoding latency is determined by the number of pipeline stages. For a fair comparison, energy and latency normalized per decoded bit, and throughput normalized by area are given at the bottom of Table I, after applying usual technology scaling rules to area, power, and throughput figures reported in the table. It can be seen that high-throughput implementations of LDPC decoders compare favorable to those of Turbo codes, for all the metrics considered.

Moreover, recent works on LDPC decoders have shown that they may accommodate imprecise computing and storage, thus enabling cost-effective, high-throughput, and/or low-power designs. The new framework of Non-Surjective Finite Alphabet Iterative Decoders (NS-FAIDs) [13] allows significant reductions of the memory and interconnect blocks of the LDPC decoder, with only slight degradation of the error correction performance. Since these blocks usually dominate the overall performance of the hardware implementation, NS-FAIDs emerge as a promising approach of high-throughput designs.

It is also worth bringing into discussion the recently discovered family of Polar codes. This has emerged as the very first construction that achieves the capacity of any binary-input memoryless output-symmetric channel, with log-linear encoding and decoding complexity. It relies on a specific recursive encoding procedure, which can be reversed at the receiver by applying a Successive CanCellation (SCC) decoder. The particularity of this construction makes Polar codes very attractive for practical applications, mainly due to their flexibility. This also explains the ongoing research effort, by both academia and industry, to investigate their use in 5G systems. However, Polar codes under SCC decoding are known to provide rather modest error correction performance at finite (short to moderate) block-lengths, as compared to the ubiquitous LDPC and Turbo codes. Several enhancements of the SCC decoder have been proposed in the literature. Although such techniques significantly improve the error correction performance in the finite block-length regime, they usually lead to an increased complexity. Besides, the sequential nature of the SCC decoder hinders the use of massively parallel architectures and results in an incompressible latency, which

may prevent deployments with significant throughput or latency constraints.

Network Architecture Modelling and Optimization

Future 5G networks will be characterized by massive deployment of mmWave small cells that will interplay with the baseline cellular network, which is needed for services that do not need very high throughput but rather robustness, mobility, and continuous coverage. These requirements cannot be satisfied by the mmWave technology that is prone to blockage and characterized by high path loss. Specifically, the coexistence and the inter-operability between microwave and 5G is currently investigated in the standardization [14].

Besides this, innovative functionalities for implementing mobility, load balancing, and radio resource management will be required. However, due to the coexistence of multiple radio access technologies, services with extremely heterogeneous requirements, and the massive density of small cell deployment, modeling, and optimizing 5G networks will be a very challenging task. In this context, stochastic geometry is emerging as a powerful tool to make the network analysis mathematically tractable. More specifically, stochastic geometry is a mathematical and statistical framework able to capture the randomness of the network topology, which has been recently extended to account for small cell deployment, directional beamforming, and mmWave path loss and blockage models [15]. However, most of the results achieved so far in this domain only modeled saturated networks, which is unrealistic and results to pessimistic performance due to the excessive interference. To deal with this, we are currently focusing on integrating queuing theory into the stochastic geometry framework in order to provide new insights on the behavior and the optimization of 5G networks.

Conclusions

The exponential growth of fixed and mobile data will be supported by mmWave technologies to provide wider data pipes. Designing mmWave systems means tackling multiple challenges such as ensuring a sufficient communication range, reducing the power consumption, and allowing the deployment of very dense networks while smartly managing the interferences. An overview of current challenges and potential enablers to move 5G mmWave communications from research to reality was proposed in this paper. The first enabler for facing the future data tsunami is the efficient usage of the Ka, V, and E bands. Looking at the signal processing standpoint, current research is focusing on the design of flexible waveforms and FEC mechanisms capable to satisfy the heterogeneous requirements of 5G services. From the technological side, the evolution of silicon technologies allows to address the mmWave communication range with low cost fully integrated solutions. When looking at small cell, advanced beam-

steering antenna that support hybrid beamforming techniques or massive MIMO are needed to maximize the radio coverage and boost the mobile communication systems. The optimization of the overall mmWave system requires novel end-to-end and hybrid software/hardware characterization, from the device to the radiation properties, as well as a holistic assessment of the network architecture performance.

Acknowledgement

References

[1] ITU-R, "Provisional Final Acts WRC-15," November 2015. http://www.itu.int/dms_pub/itu-r/opb/act/R-ACT-WRC.11-2015-PDF-E.pdf

[2] A. Siligaris et al., "A 65-nm CMOS Fully Integrated Transceiver Module for 60-GHz Wireless HD Applications," in IEEE Journal of Solid-State Circuits, vol. 46, no. 12, pp. 3005-3017, Dec. 2011.

[3] C. Dehos et al. "Millimeter-wave access and backhauling: the solution to the exponential data traffic increase in 5G mobile communications systems?," in IEEE Communications Magazine, vol. 52, no. 9, pp. 88-95, September 2014.

[4] A. Clemente, L. Dussopt, R. Sauleau, P. Potier, and P. Pouliguen, "Wideband 400-Element electronically reconfigurable transmitarray in X band," IEEE Trans. Antennas Propag., vol. 61, no. 10, pp. 5017–5027, Oct. 2014.

[5] L. Di Palma, A. Clemente, L. Dussopt, R. Sauleau, P. Potier, and P. Pouliguen, "Circularly-polarized reconfigurable transmitarray in Ka-band with beam scanning and polarization switching capabilities," IEEE Transaction on Antennas and Propag., in press.

[6] L. Di Palma, A. Clemente, L. Dussopt, R. Sauleau, P. Potier, and P. Pouliguen, "1-bit unit-cell for transmitarray applications in Ka-band," IEEE Ant. Wireless Propag. Letters, vol. 15, pp. 560–563, 2016.

[7] T. Nitsche et al., "IEEE 802.11ad: directional 60 GHz communication for multi-Gigabit-per-second Wi-Fi [Invited Paper]," in IEEE Communications Magazine, vol. 52, no. 12, pp. 132-141, December 2014.

[8] 3GPP TSG RAN, "TR 38900 Study on channel model for frequency spectrum above 6 GHz (Release 14)," V.14.1.0, September 2016.

[9] A. Bamba, F. Mani and R. D'Errico, "E-band millimeter wave indoor channel characterization," in Proc. 27th Int. Symp. Personal, Indoor and Mobile

Commun. (PIMRC'16), Valencia, Spain, Sep. 2016.

[10]   R. Gerzaguet, N. Bartzoudis, L. Gomes Baltar, et al., "The 5G candidate waveform race: a comparison of complexity and performance," EURASIP Journal on Wireless Communications and Networking, no 1, p. 13, 2017.

[11] P. Schlafer et al., "A New Dimension of Parallelism in Ultra-High Throughput LDPC Decoding", IEEE Workshop on Signal Processing Systems (SiPS), October 2013, pp. 152-158.

[12] T. Nguyen-Ly et al., "Flexible, Cost-Efficient, High-Throughput Architecture for Layered LDPC Decoders with Fully-Parallel Processing Units", Euromicro Conference on Digital System Design (DSD), September 2016, pp. 1-8.

[13] T. Nguyen-Ly et al., "Non-Surjective Finite Alphabet Iterative Decoders", IEEE International Conference on Communications (ICC), May 2016, pp. 1-6.

[14] 3GPP TSG RAN, "TR 38.804 Study on New Radio Access Technology; Radio Interface Protocol Aspects (Release 14)," V.14.0.0, August 2016.

[15] G. Gourab, A. De Domenico, and M. Coupechoux, "Modeling and Analysis of HetNets with mm-Wave Multi-RAT Small Cells Deployed Along Roads," IEEE Globecom 2017.